89-22

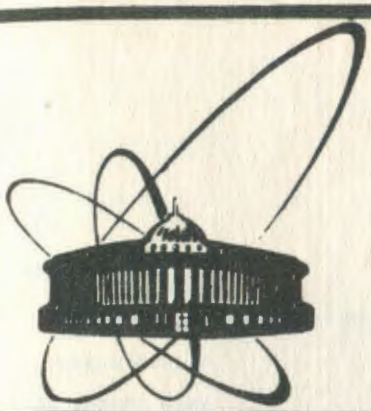

объединенный
институт
ядерных
исследований
дубна

E14-89-22

R.A.Il'khamov*, A.P.Kobzev, R.Šandrik

DEPTH PROFILING OF IRON CONCENTRATION IN Fe-Ni STRUCTURE WITH PIXE METHOD

Submitted to "Nuclear Instruments and Methods"

* Institute of Applied Physics, Tashkent State University, USSR

1989

INTRODUCTION

Non-destructive analytical techniques using ion beams have become widely used in various fields of science and technology in the recent time. Except of the bulk elemental analysis these techniques give the possibility of determining the depth concentration profiles in the near-surface region of solids.

The particle induced X-ray emission (PIXE) method can be applyed for the determination of the concentration profiles of elements at depths from 10 to 20 μm. Techniques based on the variation of both the ion beam energy [1-8] and the geometry of the experiment [9-10] have already been proposed. The main characteristics of the PIXE method are a good sensitivity to a wide range of elements combined with the possibility of distinguishing the elements having near-by atomic numbers. On the other hand the analysis of the samples consisting of near-by Z elements is sometimes hindered due to the effect of secondary excitation of a lighter element caused by the X-radiation of a heavier neighbour [11]. The secondary excitation effect in non-homogeneous samples has already been studied [12], but with the concentration of the element under determination being so small its influence on both the energy loss of incident particles and the X-ray absorption in the analysed sample could be neglected.

The present paper is devoted to the study of the depth concentration profile in a sample consisting of near-by Z elements. The PIXE method using the variation of the energy of a proton beam has been chosen for this purpose. The iron

concentration through the depth in the Fe-Ni structure has been profiling in particular.

EXPERIMENTAL

The experimental arrangement is illustrated in fig.1. The X-radiation in the analysed sample is excited by the proton beam from the Van de Graaff accelerator EG-5 of JINR. The collimated 1.5 mm in diameter proton beam interacts with a sample placed at an angle of 45° to the axis of the beam. The number of particles incident on the target is determined by charge collection using a current integrator. The X-ray yield is measured using a Si(Li)-detector installed at an angle of 90° to the axis of the beam. On the way from the sample to the detector the emitted X-rays pass through a chamber window made of Al coated Mylar foil 25 μm thick, the 10 mm thick air layer, and the 25 μm thick Be detector window. The energy resolution of the spectrometric tract was 220 eV on the 6.4 keV line of ^{57}Co isotope. The spectra compilation in external CAMAC standard memory was controlled by an MERA-60/55 minicomputer. Calculation of the areas of the K_α lines for iron and nickel was carried out with a PDP-11/70 computer using a program ACTIV [13].

An iron foil with a thickness of 50 μm covered with a 20 μm thick nickel layer was used as a sample. After thermal annealing the structure with depth concentration profile of Fe was obtained. In the process of the depth profile determination the step was chosen to be 1 μm in depth along the direction of the normal to the surface. It has been found [14] that 99% of the Ni X-ray yield is coming from the depth corresponding to 70% of the projected range of the 3 MeV protons in nickel. Taking into account this result and

Fig.1. The geometry of the experiment.

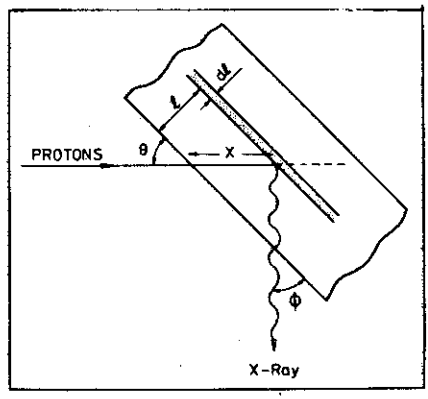

the geometry of the experiment, the energy of protons was chosen so that the change in their projected range was 2 μm per step. Energies and projected ranges of protons are presented in the table.

CALCULATION

The X-ray yield of the element under investigation without account for the secondary excitation effect can be expressed as

$$Y = Q\varepsilon \int_0^R N(x\sin\theta)\sigma(x)\exp(-\mu\rho x\sin\theta/\sin\phi)dx, \qquad (1)$$

where R is the projected range of incident protons; Q is the number of protons bombarding the target; ε is the X-ray detection efficiency including the solid angle of the detector, the absorption of X-rays on the trajectory from the target to the detector, and the detector efficiency; N is the number of atoms of the investigated element per cm^3: $N=(\rho N_o/A)C$, where N_o is the Avogadro's number, ρ is the mass density of sample (g/cm^3), A is the atomic weight of the studied element and C is the weight concentration of the element (g/g); $\sigma(x)$ the X-ray production cross section at a depth of x (cm^2); μ the mass absorption coefficient for the K_α radiation of the analysed element in the sample.

Table

N	E	R	x	Y1	Y2	Y3
1	0.719	4	2	2.79	2.77	0.55
2	0.963	6	3	11.4	11.3	2.4
3	1.190	8	4	29.4	29.2	6.99
4	1.397	10	5	57.3	56.8	16.3
5	1.563	12	6	87.1	87.3	31.2
6	1.719	14	7	134	130	65.0
7	1.870	16	8	184	175	114
8	2.020	18	9	238	223	196
9	2.171	20	10	304	279	322
10	2.323	22	11	395	341	499
11	2.474	24	12	477	406	703
12	2.622	26	13	566	470	984
13	2.766	28	14	657	525	1266
14	2.902	30	15	755	586	1611
15	3.028	32	16	854	644	1924
16	3.142	34	17	949	700	2302
17	3.243	36	18	1026	747	2613
18	3.331	38	19	1110	783	2973

N - measurement number
E - energy of proton beam, MeV
R - range of protons in nickel, μm
x - probing depth, $x=0,7R\sin\theta$, μm
Y1 - K_α X-ray yield of pure nickel, 10^{-4} (photons/proton)
Y2 - K_α X-ray yield of Ni in the analysed sample, 10^{-4} (photons/proton)
Y3 - the X-ray yield of Fe in the analysed sample, 10^{-4} (photons/proton)

The determination of the depth concentration profile of iron in the sample was carried out in the following way. Maximum probing depth in the sample was taken as a set of N layers. The iron concentration C_i in the i-th layer $[x_{i-1}, x_i]$ was assumed to be constant. The information on the depth concentration profile was evaluated on the basis of experimental Fe K_α X-ray yields $Y(E_j)$ measured at various incident proton energies $E_1, E_2, \ldots, E_N$. In this case the following system of linear equations can be written:

$$Y(E_j) = \sum_{i=1}^{j} C_i I_{ij} [1+\gamma_{ij}] \quad , \quad j=1,N. \qquad (2)$$

Here I_{ij} is the X-ray yield for iron with unity concentration in the i-th layer at the j-th energy of the beam:

$$I_{ij} = Q\varepsilon(\rho N_0/A)\int_{x_{i-1}}^{x_i} \sigma(E(E_j,x))\exp(-\mu\rho x\sin\theta/\sin\phi)dx \ ;$$

γ_{ij} is the correction for the secondary excitation of iron by K_α radiation of nickel: $\gamma_{ij} \equiv Y_{Sec,i}(E_j)/Y_{Pr,i}(E_j)$, where $Y_{Sec,i}$ and $Y_{Pr,i}$ are the yield of secondary K_α radiation of Fe excited by K_α radiation of Ni and the primary K_α radiation of Fe excited by protons in the corresponding i-th layer, respectively.

The system of equations (2) is badly conditioned since it contains both very large coefficients I_{ij} (X-ray yields from near-surface layers) as well as very small ones (X-ray yields from deeper layers). Moreover, the knowledge of the composition of each layer is necessary for the calculation of I_{ij} and γ_{ij}. Therefore, the C_i concentrations were evaluated using the following iterative scheme: at first the proposed concentration profile was chosen and theoretical X-ray yields $Y(E_j)$ calculated

for all energies E_j of the protons used in the experiment. From the comparison of the theoretical X-ray yields with the experimental ones the corrections for the concentrations C_i were inserted into the initial model. The modelling is carried out until good agreement between the theoretical and experimental dependences of the X-ray yield on proton energy is achieved. It means that the agreement of each calculated X-ray yield with the measured one must be within the experimental error of the X-ray yield.

Evaluation of the values of integrals in I_{ij} was carried out by Simpson rule. The following published data tables were used in the calculation:

- proton ranges [15] to determine the dependence of the proton energy on the penetration depth in the sample;
- X-ray production cross sections, $\sigma(E)$ [16];
- X-ray mass absorption coefficients [17].

The values of γ factor for a given geometry of the experiment at different concentrations of Fe and different proton energies were calculated using the results published in ref. [11]. The obtained dependence of γ factor on both Fe concentration and proton energy

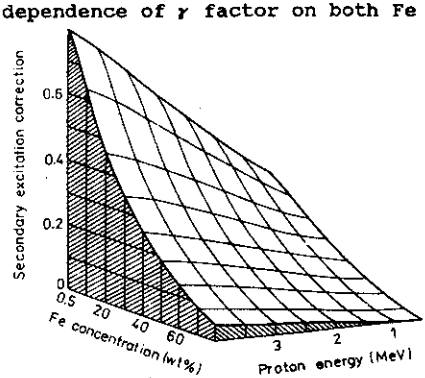

Fig.2. The dependence of the secondary excitation correction on both the Fe concentration and the proton energy.

is illustrated in fig.2. The secondary excitation correction increases with both increasing proton energy and decreasing Fe concentration.

RESULTS AND DISCUSSION

The dependences of experimental yields of K_α radiation of Fe as well as Ni on proton energy are shown in the table. For comparison the K_α X-ray yields measured with a pure nickel target are given there too.

The concentration profile of Fe in the analysed sample has been obtained by the modelling of the dependence of the experimental Fe X-ray yield on proton energy. The obtained concentration profile of Fe in the analysed sample is shown in fig.3. As can be seen from the figure, the concentration of iron is small (less than 1 wt.%) near the sample surface but it slowly approaches 100% at a depth of 5-10 μm. The absolute error of the determination of the concentration is the highest in the

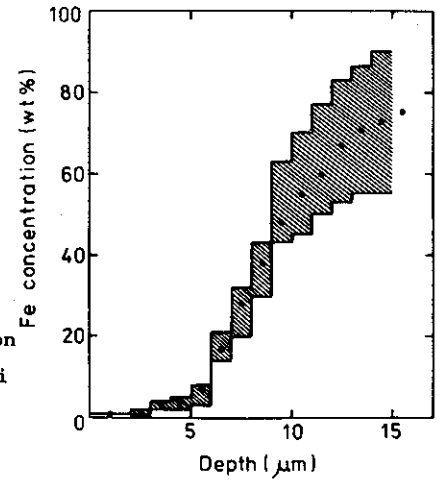

Fig.3. The depth concentration profile of Fe in the Fe-Ni structure.

deepest layers. Its increase with increasing depth can be explained by the fact that the contribution of the deepest layers to the total X-ray yield is very small.

Fig.4 shows the calculation of the relative contribution of each layer to the total K_α X-ray yield for nickel(a) and iron(b) for the proton energies used in the experiment. As can be seen from the figure, the relative X-ray yield of nickel in a selected i-th layer is not very sensitive to the energy of the proton beam (measurement number, j) except for the region of the smallest proton energies. On the other hand this relative yield for nickel is fastly decreasing with increasing depth (layer number, i) for a given energy of proton beam E_j. In contrast, the shape of the depth distribution of the relative K_α X-ray yield for iron varies significantly with increasing proton

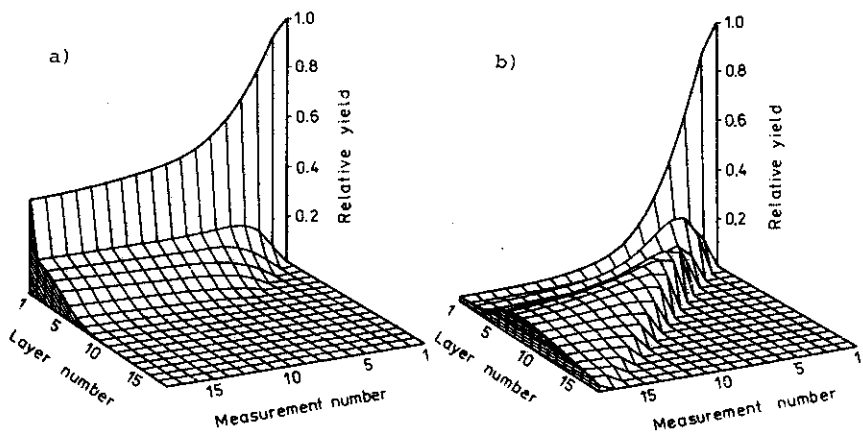

Fig.4. The corresponding to the best fit dependence of the relative contribution of each layer to the total yield of the K_α radiation of Ni(a) and Fe(b) on the proton energy (measurement number).

energy, while at higher proton energies it becomes more uniform. This fact can be explained by the character of the depth distribution of the Fe concentration. Consequently, from the obtained results the conclusion that the method allows the determination of profiles within a lower relative error in the case of increasing with depth concentration than in the case of decreasing one can be made.

Fig.5 shows the dependence of the relative difference between theoretical and experimental K_α X-ray yields of iron as well as of nickel on proton energy, $\Delta=100(Y_{calc}-Y_{exper})/Y_{calc}$. For the model of the sample corresponding to the best fit of measured yields the values of Δ for Ni are somewhat higher than the experimental error of X-ray yields (it equals 5%). A small systematic deviation of Δ values from zero in the case of Ni is perhaps due to nonsufficient accuracy account for of secondary excitation.

To have the knowledge about the sensitivity of the proposed method to a change in concentration with depth, the calculations of Δ values for a homogeneous sample model were carried out. For this purpose the following sample composition was chosen: $C_{Ni}=99.2\%$ and $C_{Fe}=0.8\%$. This composition is identical to that determined for the first layer. As can be seen from fig.5, the Δ values for Fe grow to negative values and reach -100% with increasing proton energy because in deeper layers the true concentration of iron significantly exceeds the value taken for the model. Also for Ni the values of Δ increase with increasing proton energy, but they reach only +40%. This gives an additional evidence in favor of a higher sensitivity of the PIXE technique to increasing with depth concentration profiles.

According to the obtained results it can be concluded that the PIXE method gives the possibility of determining the concentration profile in a sample consisting of near-by Z elements by applying the technique based on the variation of the energy of the proton beam and account for the secondary excitation effect.

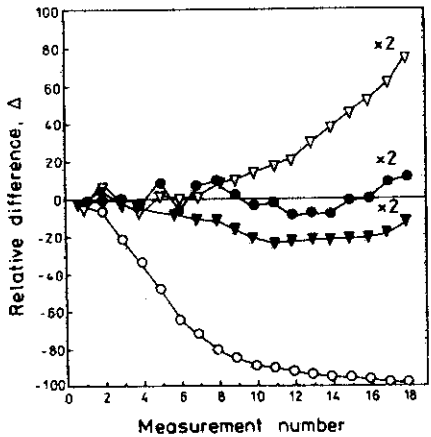

Fig.5. The dependence of the relative difference between the calculated and experimental X-ray yields, $\Delta=100(Y_{calc}-Y_{exper})/Y_{exper}$, on the proton energy (measurement number). Dark circles and triangles correspond to the concentration profiles of Fe and Ni, respectively, giving the best fit. Light circles and triangles correspond to the concentration profiles of Fe and Ni, respectively, in the model of a homogeneous sample of Ni(99.2%)-Fe(0.8%) composition.

The authors are indebted to the whole Van de Graaff accelerator staff (EG-5) of JINR for their devotion in running the accelerator.

REFERENCES

[1] F.W. Reuter and H.P. Smith , J. Appl. Phys. 43 (1972) 4228.

[2] O. Benka, M. Geretshlager and H. Paul, J. Appl. Phys. 47 (1976) 5090.

[3] O. Benka, M. Geretshlager and A. Kropf, Nucl. Instr. and Meth. 149 (1978) 441.

[4] J. Vegh, D. Berenyi, E. Koltay, I. Kiss, S. Self El-Nasr and L. Sarkadi, Nucl. Instr. and Meth., 153 (1978) 55.

[5] J. Vegh, ATOMKI Bull. 20 (1978) 229.

[6] M. Geretshlager, Nucl. Instr. and Meth. 200 (1982) 505.

[7] V. Rossiger, Nucl. Instr. and Meth. 196 (1982) 483.

[8] I. Brissaud, J.-P. Frontier and P. Regnier, Nucl. Instr. and Meth. B12 (1985) 235.

[9] W. Pabst, Nucl. Instr. and Meth. 120 (1974) 543.

[10] W. Pabst, Nucl. Instr. and Meth. 124 (1975) 143.

[11] W. Reuter, A. Lurio, F. Cardone and J.F. Ziegler, J. Appl. Phys. 46 (1975) 3194.

[12] A.R. Knudson, Nucl. Instr. and Meth. 149 (1978) 445.

[13] V.B. Zlokazov, Comput. Phys. Commun. 28 (1982) 27.

[14] R.A. Ilkhamov, Li Zen Ho, G.M. Osetinskij, M. Pajek, R.Šandrik,JINR Report, 14-86-820, Dubna, 1986.

[15] J.F. Janni, At. Data and Nucl. Data Tables 27 (1982) 341.

[16] H. Paul, Nucl. Instr. and Meth. B4 (1984) 211.

[17] E.C. Montenegro, G.B. Baptista and P.W.E.P. Duarte, At. Data and Nucl. Data Tables 22 (1978) 132.

Received by Publishing Department
on January 17, 1989.